

PROBLEM NO. NRC-3

Title: Effect of Discontinuity States on the Risk Assessment of Corroded Fuselage Lap Joints.

Objective

To illustrate the effect that different discontinuity states (initial and modified) have on a risk assessment of fuselage lap joints.

General Description

This problem focuses on: (1) the methods that can be used to investigate the statistical characteristics of different discontinuity states (DS) and (2) a risk assessment of fuselage lap joints that contain multi-site damage (MSD) and corrosion. A statistical test for homogeneity will be described, which can be used to determine if a significant difference exists between the modified discontinuity states (MDS) present in naturally corroded fuselage lap joints and those found in artificially corroded joints. A goodness-of-fit test is applied to determine the best-fit distribution for the pristine and corroded DS data. The use of the best-fit distributions for the pristine and corroded DS data in a risk assessment analysis will be described. The risk assessment program PROF (PRObability Of Fracture) is used in this problem.

Topics Covered: Corrosion, Discontinuity States (DS), Statistical Methods, Risk Assessment.

Type of Structure: Fuselage Lap Joints

Relevant Sections of Handbook: 8

Authors: Min Liao and Nicholas C. Bellinger

Company Name: National Research Council Canada
Institute for Aerospace Research
Montreal Road, Ottawa, Ontario Canada K1A 0R6
1(613) 990-9812, Website: www.nrc.ca/iar

Contact Point: Jerzy P. Komorowski

Phone: 613-993-3999

e-mail: jerzy.komorowski@nrc.ca



Overview of Problem Description

A new corrosion management approach has been proposed with the intent of anticipating, planning, and managing corrosion, which stands in sharp contrast to the present ‘find and fix’ philosophy (Peeler, 2000). This new philosophy uses the holistic (‘cradle-to-grave’) life assessment approach to address time and cyclic load issues (Brooks et al., 2000), and the cornerstone of this approach is the discontinuity state (DS) concept, which was described in detail in (Hoeppner, 1981). To characterize the different discontinuity states present in pristine (initial discontinuity state, IDS) and corroded (modified discontinuity state, MDS) fuselage lap joints, sections need to be taken from representative samples of the material, polished and the different discontinuity states that are present documented. Such a study was carried out on corroded fuselage lap joints to document the different modified discontinuity states present. The results from this study are presented in Example NRC-1 in this handbook. Experiments are also required in order to determine which of the different discontinuity states strain-energy fields (load spectrum) influence. Results from such tests are presented in Example NRC-1 in this handbook.

Due to the random nature of the different DS values, such as micro-porosity and inclusions (examples of IDS) and pit depth, intergranular cracks, exfoliation and environmentally assisted cracks (examples of MDS), a statistical analysis will be described in which a test for homogeneity and a goodness-of-fit test will be carried out. Using the results from the statistical analysis, the effect that the DS distribution has on a risk assessment of fuselage lap joints will be examined.

Coupon Test and Experimental DS values

As mentioned earlier, the experiments required to generate the DS data that will be influenced by strain-energy fields are described in Example NRC-1 in this handbook. To carry out these tests, coupons were machined from pristine, artificially and naturally corroded lap joints containing three levels of material thinning, 0%, 2% and 5% thickness loss. The holistic life approach recognizes four distinct phases of component life (nucleation, short crack, long crack, and final instability (Hoeppner and Chandrasekaran, 1998)), and requires physical discontinuity measurements and life modeling in the nucleation phase.

To determine the DS values for the different corrosion levels, the majority of the fracture surfaces from the pristine, 2% artificial and 2% natural coupons were examined with the aid of a scanning electron microscope (SEM). For the pristine coupons the nucleation sites were located along the non-machined edge while for the corroded coupons, they were located along the corroded faying surface edge. Although all the nucleation sites were semi-elliptical in shape, a semi-circular crack was used to describe the DS with an equivalent area to the initial semi-elliptical crack. It should be pointed out that the equivalent corrosion damage (ECD) defined in Example NRC-1 of this handbook corresponds to the MDS values in the holistic life assessment approach.

To verify the ability of the DS concept to predict the life of each coupon, the AFGROW crack growth program was used to predict the number of cycles to failure, which were then compared to the particular experimental result of the corresponding coupon (Bellinger et al., 2001). The results showed that all the predicted cycles to failure were within 10% of the experimental results (the largest error occurred when multiple nucleation sites were present in the coupons). This

good correlation indicated that the DS values could be back calculated from the number of cycles to failure of the coupons using the AFGROW program. Therefore, the DS data for the 5% corroded coupons, were determined by back calculations.

To compare the different DS data without knowing the best-fit distribution, each set of DS samples was ranked and their empirical distribution functions (EDFs) plotted as shown in [Figure NRC-3.1](#). As can be seen from this figure, there is distinct difference between the EDFs of the 2% and 5% corrosion DS samples while for the pristine and 2% corrosion, the difference is relatively small. The mean and standard deviations of all the DS samples are presented in [Table NRC-3.1](#).

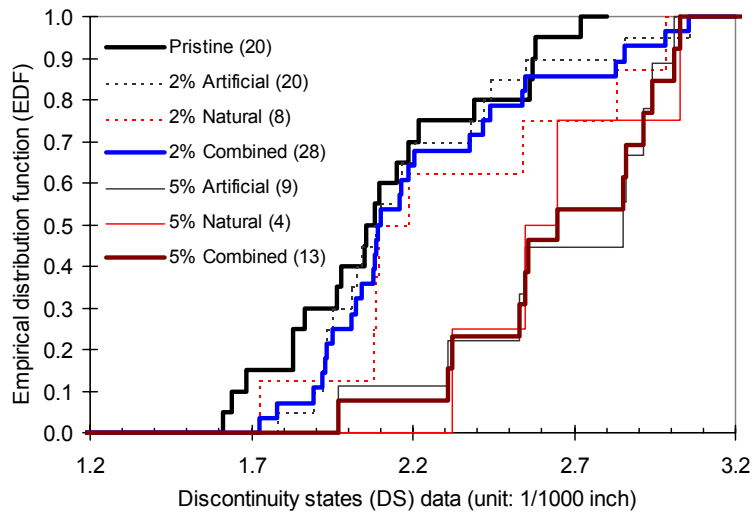


Figure NRC-3.1. Empirical distribution function (EDF) of DS data, () denotes sample size.

Table NRC-3.1. IDS and MDS values.

	IDS Pristine (inch)	Artificial MDS 2% (inch)	Natural MDS 2% (inch)	Combined MDS 2% (inch)	Artificial MDS 5% (inch)	Natural MDS 5% (inch)	Combined MDS 5% (inch)
Mean	0.002103	0.002194	0.002314	0.002229	0.002659	0.002638	0.002652
Std. dev.	0.0003265	0.0003322	0.0004291	0.0003584	0.0003479	0.0002959	0.0003204
Coefficient of variation	15.52%	15.14%	18.54%	16.08%	13.08%	11.22%	12.08%
Sample size	20	20	8	28	9	4	13

Statistical Characteristics of DS data

Test for homogeneity of artificial and natural MDS samples

Although the sample size is small for each set of DS data generated, combining the natural and artificial results could increase it. However, before this can be accomplished, a test for homogeneity based on the k-sample Anderson-Darling statistic, which is recommended in MIL-HDBK-17 and 5 (Department of Defense, 1997, 1998) must first be carried out. This test is used

to determine whether a significant difference exists between two samples (in this case artificial and natural corrosion MDS samples) so that they could be pooled together to get a larger sample.

[Table NRC-3.2](#) presents the k-sample Anderson-Darling test results for the artificial and natural MDS samples for the 2% and 5% corrosion levels. This table shows that the hypothesis that the artificial and natural MDS samples, either for the 2% or 5% corrosion, are from the same population was not rejected at a significance level (SL) of 5%. In addition, a previous study (Eastaugh et al., 2000) has shown that the physical appearance and microscopic topography of the damage from artificially and naturally corroded lap splices were similar. Based on these results, it was concluded that there was no significant difference in the damage resulting from the accelerated corrosion process as compared to the damage associated with the natural process. Therefore, the two MDS samples were combined, and the mean and standard deviation of the combined MDS data are also presented in [Table NRC-3.1](#). [Figure NRC-3.1](#) also shows the EDF of the combined MDS data for the 2% and 5% corrosion.

Table NRC-3.2. k-sample Anderson-darling test results.

Sample data	Homogeneity hypothesis	ADK (MIL-HDBK-17, 5)	Critical value of ADK	Conclusion
2% artificial and natural MDS samples	Two samples are from the same population	0.66	2.40	can not reject at SL=5%
5% artificial and natural MDS samples	Two samples are from the same population	0.49	2.30	can not reject at SL=5%

Best-fit distributions of DS data

Except for the 5% corrosion MDS data, the majority of the DS data were measured from the fracture surfaces with the aid of a SEM. Generally, in a material degradation process, failure may depend on the strength of the weakest element, or it may depend on the largest crack-like discontinuity present in the material. Therefore, it is reasonable to assume that the DS values used in this example are the largest values among all discontinuities. Based on the physical behavior of the DS, the mathematical simplicity as well as the usability in engineering (Liao et al., 2001b), six continuous distributions, presented in [Table NRC-3.3](#), were selected as alternative (candidate) distributions to describe the DS data.

Table NRC-3.3. Alternative distributions.

No	Distribution form	Distribution function	Domain of variable
1	Normal	$F(x) = \Phi[(x - \mu) / \sigma]$	$x \in (-\infty, +\infty)$
2	Lognormal	$F(x) = \Phi[(\ln x - \mu) / \sigma]$	$x \in (0, +\infty)$
3	Weibull	$F(x) = 1 - \exp[-(x / \alpha)^\beta]$	$x \in [0, +\infty)$
4	Type-I extreme value distribution (EVD) of smallest values	$F(x) = 1 - \exp\{-\exp[(x - a) / b]\}$	$x \in (-\infty, +\infty)$
5	Gumbel (Type-I EVD of largest values)	$F(x) = \exp\{-\exp[-(x - a) / b]\}$	$x \in (-\infty, +\infty)$
6	Frechet (Type-II EVD of largest values)	$F(x) = \exp[-(\alpha / x)^\beta]$	$x \in [0, +\infty)$

In this example, all the alternative distributions were tested to fit the pristine, combined 2%, and combined 5% corrosion MDS data. Anderson-Darling goodness-of fit (A-D GOF) test (Department of Defense, 1997, 1998) was used to quantitatively examine which distribution

could provide the best fit to the DS data. All the parameters for the six alternative distributions were estimated using the maximum likelihood estimators (MLEs) (Liao et al., 2001b). The results showed that:

1. For the pristine IDS data, the Gumbel, Lognormal, Frechet, and Normal distributions were *highly acceptable* (significance level, $SL > 20\%$), the Weibull distribution was *acceptable* ($5\% < SL < 20\%$), and only the Type-I EVD of smallest values was *unacceptable* ($SL < 5\%$);
2. For the combined 2% MDS data, the Frechet and Gumbel distributions were *highly acceptable*, and the other alternative distributions were all *unacceptable*;
3. For the combined 5% MDS data, Type-I EVD of smallest values, Weibull, and Normal distributions were *highly acceptable*, the Gumbel distribution was *acceptable*, and only the Frechet was *unacceptable*;
4. Only the Gumbel distribution was *acceptable* for all the DS data sets.

Another method to determine which distribution describes the data best is to plot the different distributions on a probability paper. This example plotted the six alternative distributions and the DS data on Normal probability papers, and the results are shown in [Figures NRC-3.2 to NRC-3.4](#) for the pristine, combined 2%, and combined 5%, respectively. The symmetrical ranks (Shimokawa and Liao, 1999); i.e., $p_i = (i - 0.5) / n$, were used as the plotting positions for the DS data. After carefully examining these plots, the same conclusions from the A-D GOF test could be drawn. It should be emphasized that the goodness-of-fit test and the probability plot are complementary to each other and both should be used to determine the best-fit distribution.

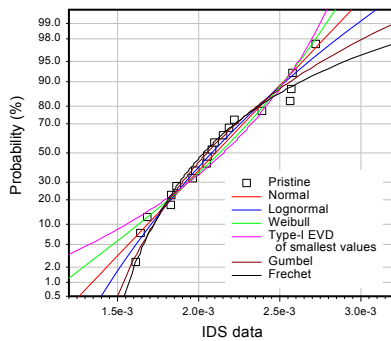


Figure NRC-3.2. Pristine IDS data plot on Normal probability paper

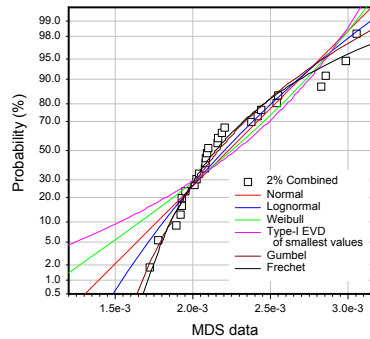


Figure NRC-3.3. Combined 2% MDS data plot on Normal probability paper.

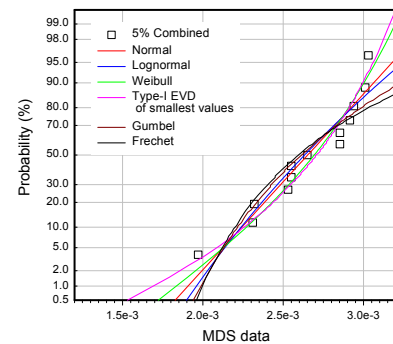


Figure NRC-3.4. Combined 5% MDS data plot on Normal probability paper.

Risk Analysis of Fuselage Lap Joints

MSD corrosion/fatigue test

Tests were carried out on multi-site damage (MSD) lap splice specimens to determine the effect that corrosion has on the fatigue life of a longitudinal fuselage lap joint (Eastaugh et al., 2000). [Figure NRC-3.5](#) shows a schematic of the specimen, which was constructed of two 1.0 mm (0.040 inch) sheets of 2024-T3 clad aluminum with three rows of 4 mm (5/32 inch) 2117-T4 countersink rivets. Specimens were pre-corroded using an accelerated corrosion process. Three

corrosion levels were examined: 0%, 2%, and 5% average material loss. Fatigue tests were then performed by applying a constant amplitude loading such that the stress approximately one inch away from the critical rivet row was 98.5 MPa (14.3 Ksi) with a stress ratio of 0.02 and a frequency of 8 Hz .

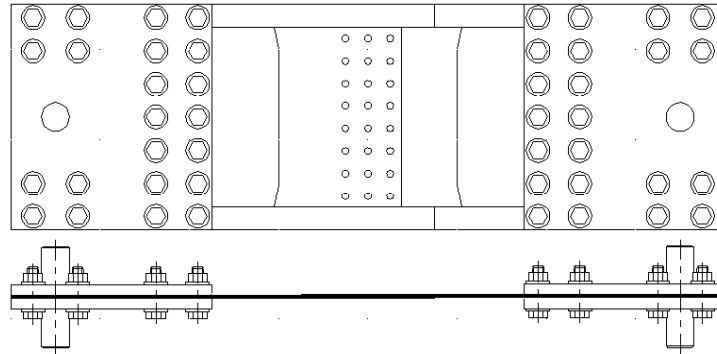


Figure NRC-3.5. Schematic of the MSD specimen.

Examinations of the failed specimens revealed that the majority of the crack nucleation sites were located away from the rivet hole along the faying surface and were semi-elliptical in shape. Although different MSD scenarios were observed in the pristine and corroded MSD tests, the onset of MSD, that is life to visible cracks, occupied over 80% of the total life and thus was used as the failure criteria for the risk analysis. The probability of failure (POF) for the onset of MSD in both the pristine and corroded specimens was predicted using the computer code, PROF (PRobability Of Fracture) (Berens et al., 1991) (Hovey et al., 1998). PROF has been used for quantifying risk and cost associated with inspection, replacement, and retirement of aging aircraft. The input data was found to play a key role in obtaining accurate POF predictions (Liao and Xiong, 2001a) (Liao and Xiong, 2000).

Input data preparation for PROF

Initial crack size distribution (ICSD) – To investigate the influence of the DS distributions on the POF predictions, all the *acceptable* distributions were used as ICSD in the risk analysis. Since PROF required a tabular format for the ICSD input, i.e., $(a_i, F(a_i))$, 1000 points of $(a_i, F(a_i))$ data were generated based on the distribution function and estimated parameters (Liao et al., 2001b).

Median crack growth curve – The crack growth analysis of pristine and corroded lap joints was accomplished earlier using the classic model of a corner crack at a straight hole in AFGROW (Bellinger et al., 2001). Stress correction factors, generated using a three dimensional finite element analysis, were used to take into account the bending, bearing, and corrosion pilling that occur in non-corroded and corroded lap joints. Material thinning for the corroded joints was also taken into account by increasing the remote stress by the appropriate amount. Using the methods of (Bellinger et al., 2001), the median crack growth $(a-N)$ curves for pristine and corroded lap joints were obtained, which are shown in [Figure NRC-3.6](#). One hundred points of tabular (a_i, N_i) data were used in PROF.

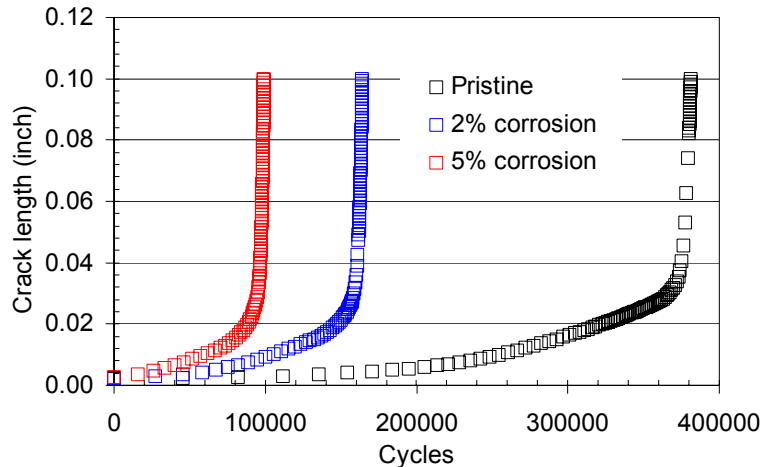


Figure NRC-3.6. Calculated a - N curves for pristine and corroded MSD specimens.

Critical crack length – In this example, a visible crack length of 2.54 mm (0.1 inch), i.e., the onset of MSD, was taken as the critical crack length for both the pristine and corroded specimens. This crack length was measured from the edge of the hole as it emerged beyond the rivet head on the outer skin of the specimen and was chosen because it was small enough not to be influenced by an adjacent crack.

Fracture toughness distribution and geometry factor – For the 1.0 mm (0.04 inch) sheet of 2024-T3 clad aluminum, the fracture toughness distribution was assumed to follow a normal distribution with a mean and standard deviation of 151.6 MPa \sqrt{m} (138.0 Ksi \sqrt{in}) and 5.5 MPa \sqrt{m} (5.0 Ksi \sqrt{in}), respectively (The Boeing Company, 1998). Since this analysis defined a small critical crack length, the fracture toughness criterion had no influence on the risk analysis. The input of the fracture toughness distribution was needed to run the software. For the same reason, the geometry factors were also arbitrarily set to be small values so that the fracture toughness criterion would not affect the calculated results.

Maximum stress distribution – The Gumble distributions with a mean at the constant amplitude level in the test and a small standard deviation were used for the maximum stress distribution. Using the method of (The Boeing Company, 1998), the Gumble parameters for the pristine and corroded specimens were calculated by taking into account the material loss due to corrosion. Since the critical crack length criterion was applied in this example, the maximum stress distribution had an insignificant effect on the risk analysis.

Probability of detection, $POD(a)$, and repaired crack size distribution (RCSD) – Since this risk analysis does not involve any inspection or repair activities, arbitrary but reasonable data were used to define the $POD(a)$, and the RCSD.

Comparison of analytical and test results

Figures NRC-3.7 and NRC-3.8 show the results from the POF predictions for the pristine and corroded specimens. The experimental results, which were ranked and also plotted in these figures, used the symmetrical ranks as the plotting positions. The experimental results, which as mentioned earlier was the number of cycles to visible cracks, were observed from the central

four holes of the top rivet row and resulted in a sample size of 18, 7, and 1 for the pristine, 2%, and 5% corroded specimens, respectively.

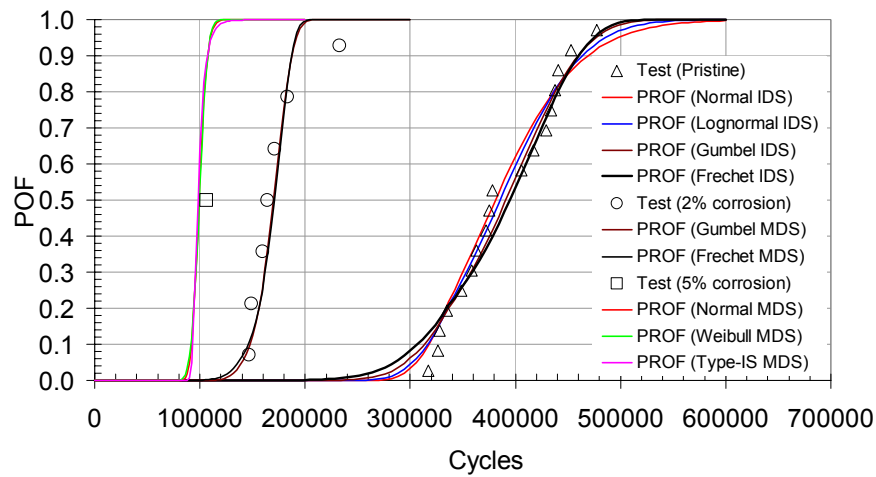


Figure NRC-3.7. POF predictions for pristine and corroded MSD specimens using the *highly acceptable* DS distributions.

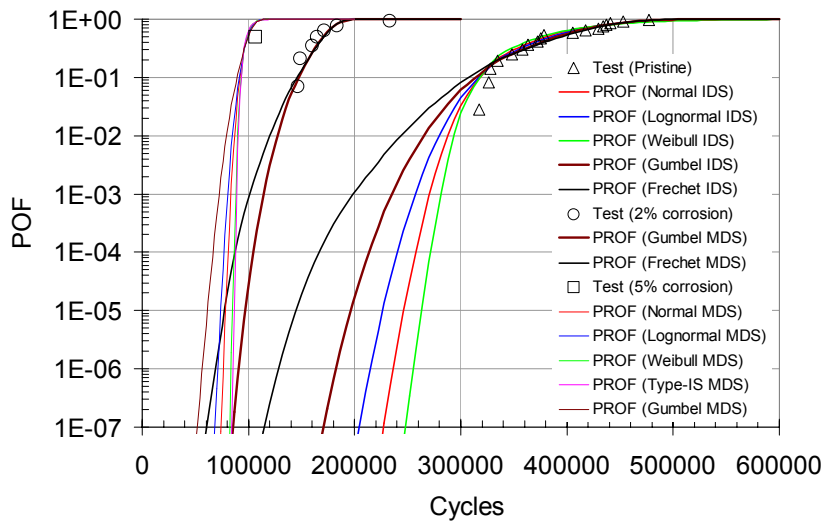


Figure NRC-3.8. POF predictions for pristine and corroded MSD specimens using the *acceptable* DS distributions.

[Figure NRC-3.7](#) presents the POF predictions for the pristine and corroded specimens using different *highly acceptable* (best-fit) DS distributions. The results from [Figure NRC-3.7](#) indicate that:

- For the pristine and 2% corroded specimens, predictions are close to the test results. Again A-D GOF tests (distribution free GOF test (Lawless, 1982)) were carried out and indicated that the predictions fit the test results very well (all $SL > 15\%$). All best-fit DS distributions produced close POF results to each other, especially for the corroded specimens;

- For the 5% corroded specimens, the prediction can't be compared to the test result since there is only one test datum available, however, the predicted mean life is close to this test datum;
- The POF results for the 2% corroded specimens are much higher than those for the pristine specimens, that is, corrosion in lap joints, even at low thickness loss levels, can result in a great increase of the POF. From the predictions, the POF difference between 2% and 5% is less than that between the pristine and 2%. This is consistent with the finding that the corroded surface topography at 5% may be “smoother” than that at 2% (Bellinger et al., 2000).

[Figure NRC-3.8](#) presents the POF predictions for the pristine and corroded specimens using the *acceptable* DS distributions and is shown in logarithmic scale to more easily distinguish the results in the low probability zone (<0.1). Although the test data did not have a large enough sample size to verify the predictions in the low probability zone, [Figure NRC-3.8](#) does reveal the following:

- For the pristine specimens, the different DS distributions produced significantly different POF predictions in the low probability zone. Assuming that 10^{-7} is an acceptable risk level for maintenance scheduling (Lincoln, 2000), the Frechet DS distribution gave the shortest time while the Weibull DS distribution gave the longest time and the time difference was about 130,000 cycles.
- For the 2% corroded specimens, the different MDS distributions also produced different POF predictions in the low probability zone, though the difference was not as significant as in the pristine case. However, the maintenance schedule could be significantly shortened due to prior corrosion even at this low thickness loss level. In this example, at a risk level of 10^{-7} , the time difference between the pristine and 2% corrosion cases was about 9,000 cycles, according to the POF predictions produced by the Gumbel DS distribution.

[Figure NRC-3.8](#) also shows that the POF curves for the corroded specimens in the low probability zones are “steeper” than the curve for the pristine results, given the same type of DS distribution, for example the Gumbel distribution. This steeper curve would have a profound effect on the probability of failure if corrosion was missed during routine inspections. [Figure NRC-3.9](#) illustrates an example, in which a risk assessment was carried out to maintain a POF level under 10^{-7} using the Gumbel DS distribution for both the pristine and corroded specimens and a log-logistic distribution (Berens et al., 1991) was assumed for the POD(a) with $\mu=0.01$ and $\sigma=0.1$. To maintain the acceptable POF level for the pristine specimens, the first inspection would have to be carried out at 170,000 cycles, while the second inspection would be required at about 236,000 cycles. If during the first inspection, 5% corrosion was missed, this would significantly increase the POF at the second inspection interval by three orders of magnitude (10^4). [Figure NRC-3.9](#) also shows that a risk assessment can aid in scheduling the maintenance associated with corrosion. This assessment could allow a corroded lap joint to remain in service until the next scheduled maintenance while maintaining the acceptable POF level.

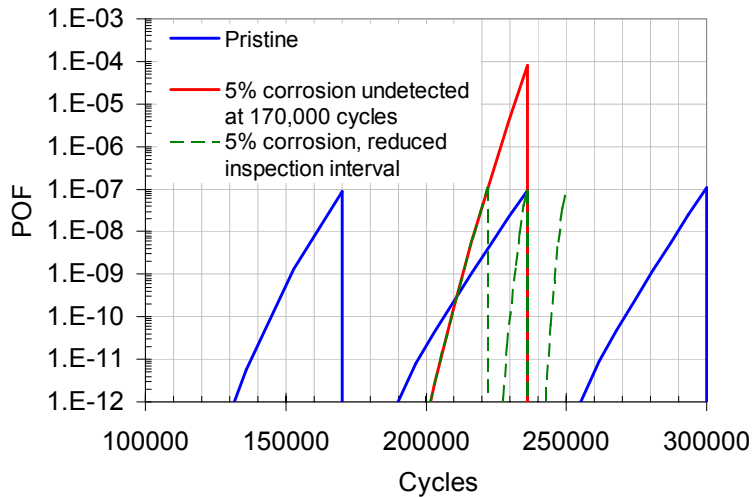


Figure NRC-3.9. Corrosion risk assessment example: what-if scenario predictions.

References

Bellinger, N.C., Cook, J.C. and Komorowski, J.P. (2000), “The Role Of Surface Topography In Corroded Fuselage Lap Joints”, The proceedings of the 2000 USAF Aircraft Structural Integrity Program Conference, San Antonio, Texas, 2000.

Bellinger, N.C., Komorowski, J.P. and Benak, T.J. (2001), “Residual Life Predictions Of Corroded Fuselage Lap Joints”, International Journal of Fatigue, Vol.23, No. 11, pp. 349-356, 2001.

Berens, A.P., Hovey, P.W. and Skinn, D.A. (1991), “Risk Analysis For Aging Aircraft, Vol.1—Analysis”, WL-TR-91-3066, Air Force Research Laboratory, Wright-Patterson Air Force Base, Ohio, 1991.

The Boeing Company (1998), D500-13008-1, Corrosion Damage Assessment Framework, Seattle, W.A., 1998.

Brooks, C., Honeycutt, K., and Prost-Domasky, S. (2000), “Case Studies For Life Assessments With Age Degradation”, The proceedings of the Fourth Joint DoD/FAA/NASA Conference on Aging Aircraft, St. Louis, Missouri, May, 2000.

Department of Defense (1997) MIL-HDBK-17E, Polymer Matrix Composites. Vol.1, U.S.A.

Department of Defense (1998) MIL-HDBK-5H, Metallic Materials and Elements for Aerospace Vehicle Structures, U.S.A.

Eastaugh, G.F., Straznicky, P.V., Krizan, D.V., Merati, A.A. and Cook, J. (2000), “Experimental Study Of The Effects Of Corrosion On The Fatigue Durability And Crack Growth

Characteristics Of Longitudinal Fuselage Splices”, Proceeding of the Fourth DoD/FAA/NASA Aging Aircraft Conference. St. Louis, 2000.

Hoepfner, D.W., (1981), “Estimation of Component Life by Application of Fatigue Crack Growth Threshold Knowledge”, Fatigue, Creep and Pressure Vessels for Elevated Temperature Service: presented at the Winter Annual Meeting of the American Society of Mechanical Engineers, Washington, D.C., edited by Carl W. Lawton, R. and Rodger Seeley, sponsored by the Metal Properties Council, Inc., the Materials Division, ASME, pp. 1-84, 1981.

Hoepfner, D.W. and Chandrasekaran, V. (1998), “Corrosion And Corrosion Fatigue Predictive Modeling State Of The Art Review”, submitted as a part of the research program “*Modeling Corrosion Growth on Aircraft Structure*” subcontract Number NCI USAF 9061-008, April 30, 1998.

Hovey, P.W., Berens, A.P. and Loomis, J.S. (1998), “Update Of The PROF Computer Program For Aging Aircraft Risk Analysis, Vol.1- Modifications And User’s Guide”, UDR-TR-1998-00154, Air Force Research Laboratory, Wright-Patterson Air Force Base, Ohio, 1998.

Lawless, J.F. (1982), Statistical Models And Methods For Lifetime Data. John Wiley & Sons, New York, 1982.

Liao, M. and Xiong, X. (2000), “Risk Assessment Of Aging Aircraft Structures Using PRISM and PROF”, Canadian Aeronautics and Space Institute Journal, Vol. 46, No. 4, pp. 191-203, 2000.

Liao, M. and Xiong, Y. (2001a), “A Risk Analysis Of Fuselage Splices Containing Multiple Site Damage And Corrosion”, Journal of Aircraft, Vol. 38, No. 2, pp. 181-187, 2001.

Liao, M., Bellinger, N., and Komorowski, J.P. (2001b), “Statistical Characteristics Of Discontinuity States And Their Application To Corrosion Risk Assessment Of Aircraft Structures”, Proceedings of ICAF 2001, Toulouse, France, June 2001.

Lincoln, J.W. (2000), “Effect Of Aircraft Failures On USAF Structural Requirements”, Proceeding of ICAS 2000, England.

Peeler, D. (2000), “Managing The Impact Of Environment Degradation On The USAF Fleet”, The proceedings of the Fourth Joint DoD/FAA/NASA Conference on Aging Aircraft, St. Louis, Missouri, May, 2000.

Shimokawa, T. and Liao, M. (1999) “Goodness-of-Fit Tests for the Type-I Extreme-Value and Two-Parameter Weibull Distributions”, IEEE Transactions on Reliability, Vol. 48, No.1, pp. 79-86, 1999.